

Research Article

Graphene oxide–TiO₂ composite materials for photocatalytic degradation of organic pollutants in water treatment

Caroliny Fernandes de Carvalho , Adhimar Flávio Oliveira , Maria Elena Leyva Gonzalez , Vander Alkmin dos Santos Ribeiro* , Celso Henrique Correa Carvalho

ABSTRACT: The increasing presence of recalcitrant organic pollutants in water bodies has driven the development of advanced treatment technologies capable of promoting effective degradation beyond conventional processes. In this study, a graphene oxide (GO)–titanium dioxide (TiO₂) composite was synthesized via a chemical route and evaluated for photocatalytic degradation of methylene blue under UVC irradiation. Graphene oxide was produced by electrochemical exfoliation of graphite, followed by incorporation into TiO₂ at 5 wt.% to form the TiO₂:GOS composite. Structural and morphological characterizations by X-ray diffraction, scanning electron microscopy, energy-dispersive X-ray spectroscopy, and FTIR confirmed the formation of anatase-phase TiO₂ and successful integration of GO without secondary phase formation. Photocatalytic performance was assessed by monitoring dye concentration decay over 5 h of irradiation. The TiO₂:GOS composite achieved more than 70% methylene blue removal, reaching a final C/C₀ value of 0.28, compared to 0.29 for pure TiO₂ under identical conditions. The degradation followed pseudo-first-order kinetics, with apparent rate constants of $2.302 \times 10^{-1} \text{ h}^{-1}$ for the composite and $2.241 \times 10^{-1} \text{ h}^{-1}$ for pure TiO₂, corresponding to a 2.7% increase in reaction rate. Enhanced initial adsorption and slightly faster absorbance decay were observed for the composite throughout the irradiation period. Although the performance enhancement is moderate, the incorporation of graphene oxide improved charge separation and adsorption behavior without requiring high-temperature calcination. These findings demonstrate that GO modification represents a viable strategy to enhance TiO₂ photocatalytic activity under energy-efficient synthesis conditions, highlighting its potential application in advanced water and wastewater treatment systems.

Keywords: Graphene oxide–TiO₂ composite, Photocatalytic degradation, Advanced oxidation processes, Organic pollutants, Environmental remediation

1. INTRODUCTION

Population growth, accelerated urbanization, and the intensification of industrial activities have collectively contributed to a substantial increase in effluent generation and the contamination of water bodies by diverse organic pollutants, including dyes, pharmaceuticals, pesticides, and aromatic compounds [1]. These anthropogenic pressures pose significant threats to aquatic ecosystems and human health.

In this context, water treatment plants (WTPs) and wastewater treatment plants (WWTPs) play a critical role in safeguarding public health and environmental integrity. These facilities are designed to remove physical, chemical, and biological contaminants from water before it is released for human consumption or discharged into natural water bodies [2, 3]. The effectiveness of these treatment systems is therefore essential for maintaining water quality standards and preventing the propagation of waterborne pollutants.

Despite the efficiency of conventional processes employed in water and wastewater treatment plants, such as coagulation, flocculation, sedimentation, filtration, and biological treatments, many recalcitrant organic pollutants are not completely removed by these technologies [4]. According to Morin et al. (2021) [1], recent literature widely confirms that urbanization, industrialization, and intensive agri-

OPEN ACCESS

Affiliation

Universidade Federal de Itajubá (UNIFEI), Av. BPS, 1303, Itajubá, Minas Gerais, 37500-903, Brazil

*Correspondence

Email: vanderalkmin@gmail.com

ORCID

Caroliny Fernandes de Carvalho: 0009-0003-3657-6095

Adhimar Flávio Oliveira: 0000-0003-2586-7359

Maria Elena Leyva Gonzalez: 0000-0003-0673-5713

Vander Alkmin dos Santos Ribeiro: 0000-0003-0260-2454

Celso Henrique Correa Carvalho: 0000-0001-7667-6961

Received: February 9, 2026

Revised: February 25, 2026

Accepted: February 28, 2026

How to cite: de Carvalho, C., F., Oliveira, A., F., Gonzalez, M., H., L., Ribeiro, V., A., dos S., Carvalho, C., H., C., (2026). Graphene oxide–TiO₂ composite materials for photocatalytic degradation of organic pollutants in water treatment. *Journal of Applied Materials and Technology*, 7(2), 74–84. <https://doi.org/10.31258/Jamt.7.2.74-84>.

Copyright (c) 2026 Caroliny Fernandes de Carvalho, Adhimar Flávio Oliveira, Maria Helena Leyva Gonzalez, Vander Alkmin dos Santos Ribeiro, Celso Henrique Correa Carvalho. This article is licensed under a [Creative Commons Attribution 4.0 International License](https://creativecommons.org/licenses/by/4.0/).



culture significantly increase the load of emerging organic contaminants in water bodies, and conventional treatment plants were not designed to fully remove them. Persistent organic compounds, including synthetic dyes and emerging micropollutants, may pass through treatment systems and reach receiving water bodies, causing environmental and ecotoxicological impacts. This limitation has driven the search for complementary or advanced treatment technologies capable of promoting the effective degradation of these contaminants.

Within this scenario, advanced oxidation processes stand out as promising alternatives for application in water and wastewater treatment plants, as they enable the degradation of organic pollutants through the generation of highly reactive species, such as hydroxyl radicals. Among advanced oxidation processes, heterogeneous photocatalysis has received increasing attention due to its efficiency, environmental feasibility, and potential for integration into existing treatment systems. Heterogeneous photocatalysis is considered attractive because of its high efficiency in degrading a wide range of contaminants, its environmental viability, since it does not require continuous addition of chemical reagents and can employ solar energy, and its potential integration into existing treatment systems, where it can operate as a complementary step or as a final polishing stage in water and wastewater treatment plants [5, 6].

Titanium dioxide (TiO_2) is widely studied as a photocatalyst for environmental applications due to its chemical stability, low cost, and non-toxicity. However, inherent limitations of TiO_2 , such as the rapid recombination of electron-hole pairs and low absorption in the visible region, reduce its efficiency in degrading organic pollutants present in treated water and wastewater [7]. To overcome these limitations, the formation of composites with carbon-based materials, such as graphene oxide, has been investigated. Graphene oxide exhibits a high specific surface area and oxygen-containing functional groups that favor the adsorption of organic contaminants, in addition to contributing to improved separation of photogenerated charges, which is an essential aspect for environmental applications in water and wastewater treatment systems [8].

The scope of this work focuses on the development of a graphene oxide and TiO_2 composite obtained via chemical synthesis, with emphasis on its application in the photocatalytic degradation of organic pollutants, aiming at potential use as a complementary technology in water and wastewater treatment plants [9]. Graphene oxide is obtained from commercial graphite using a chemical method adapted from Hummers, while TiO_2 is synthesized under controlled conditions, seeking a material with structural and morphological properties suitable for environmental treatment processes [10, 11]. The efficiency of the composite is evaluated through the degradation of the methylene blue dye, used as a model compound to simulate organic pollutants present in liquid effluents. The research problem guiding this study consists of verifying whether a graphene oxide and TiO_2 composite obtained through a conventional chemical route exhibits adequate photocatalytic performance for the degradation of organic pollutants resistant to conventional treatments employed in water and wastewater treatment plants. The analysis of this performance is essential to assess the feasibility of the material as an alternative or complementary step in existing treatment systems. The overall ob-

jective of this work is to develop and evaluate a graphene oxide and TiO_2 composite with potential application in water and wastewater treatment plants, aiming at the photocatalytic degradation of organic pollutants. The relevance of this study lies in its contribution to the development of photocatalytic materials applicable to advanced water and wastewater treatment, especially as a complementary technology in water and wastewater treatment plants.

2. METHODOLOGY

2.1. Materials. GO was synthesized by electrochemical exfoliation of graphite using a two-electrode cell, following the procedure reported by Pereira et al. (2023) [12]. The experiment was carried out using two commercial graphite electrodes with dimensions of 7.0 mm \times 7.0 mm, connected to the positive and negative terminals of an Instrutherm FA 3005 power supply.

2.2. Synthesis. The electrodes were arranged in parallel and partially immersed in a 1 mol L⁻¹ sulfuric acid (H_2SO_4) solution, prepared using Neon reagent with purity between 95% and 98%. This electrolytic medium was used both for GO synthesis and for the preparation of TiO_2 :GO composites.

After the addition of 120 mL of the H_2SO_4 solution, an initial potential difference of 3 V was applied for 10 minutes. Subsequently, voltages of 7 V, 9 V, and 11 V were applied sequentially, each for a period of 5 minutes. At the end of the electrochemical process, the obtained material was subjected to successive washing steps with distilled water by filtration. After each washing step, the pH was monitored using indicator strips until a neutral pH was reached. The resulting material was then dried in an oven at 100 °C for 24 hours. For the preparation of TiO_2 :GO composites, 2 mL of titanium tetrabutoxide ($\text{Ti}(\text{OC}_4\text{H}_9)_4$, Sigma Aldrich, purity \geq 99%) was added to three separate beakers. Subsequently, masses of 0.000 g, 0.050 g, and 0.100 g of graphene oxide were incorporated, corresponding to 0% and 5% by mass of GO, respectively. The composition containing 5% GO (TiO_2 :GO5) was defined based on the mass ratio between graphene oxide and TiO_2 , corresponding to 5 wt.% of GO in relation to TiO_2 .

To each system, 30 mL of ethanol (ethyl alcohol, purity \geq 99.5%, Sigma Aldrich) was added. Titanium tetrabutoxide was used as the precursor of titanium dioxide (TiO_2), responsible for the formation of the inorganic matrix of the composites. Ethanol acted as both a solvent and a hydrolysis rate-controlling agent, favoring the formation of more homogeneous mixtures. Graphene oxide, incorporated in different proportions, was intended to evaluate its influence on the structure and properties of the composites, considering the presence of oxygen-containing functional groups on its surface, which favor interactions with TiO_2 .

After solution preparation, the three samples were subjected to an evaporation process to remove the solvent and promote TiO_2 formation. For this purpose, the contents were transferred to a round-bottom flask containing small glass beads, aiming to ensure homogeneous heat distribution during heating. The system consisted of a flask coupled to a heating mantle, a condenser, and a Dean Stark apparatus with two joints, operating at the boiling temperature of ethanol. After completion of the synthesis process, the composites were filtered with distilled water using a funnel and filter paper and subsequently allowed to dry. After this step, the samples were stored in 1.5 mL microtubes for subsequent characterization

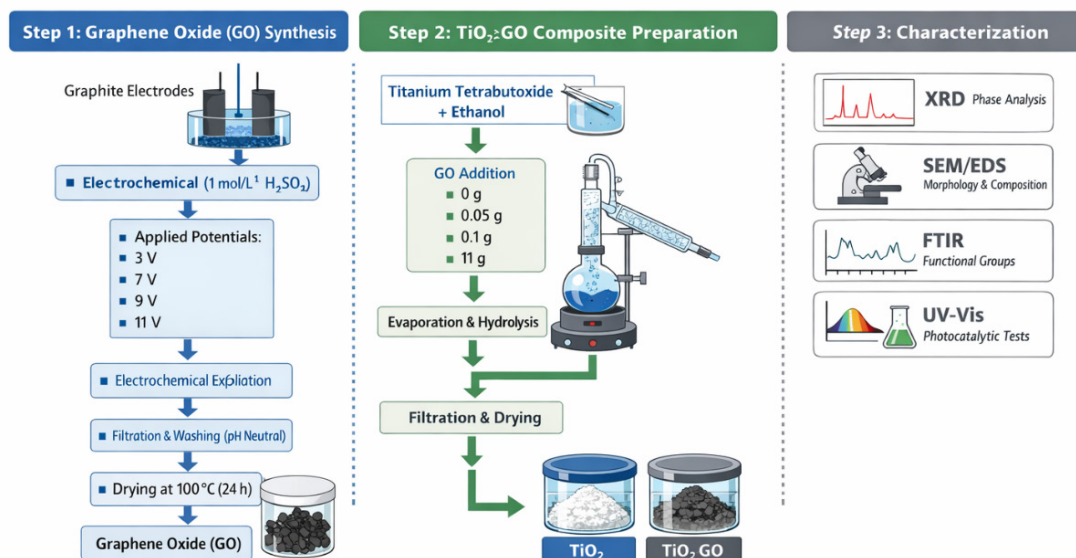


Figure 1. The diagram provides a clear and reproducible overview of the experimental procedure.

2.3. Characterization. Structural analysis of the materials was performed by X-ray diffraction (XRD) using a high-resolution X'Pert PRO diffractometer from PANalytical. The diffraction patterns were obtained using Cu K α radiation with $\lambda = 1.5406 \text{ \AA}$, in the 2θ range from 5° to 90° , with an angular step of 0.02° and an acquisition time of 2 seconds per step.

Morphological characterization of the materials was carried out by scanning electron microscopy (SEM) using a Carl Zeiss EVO MA 15 microscope. Elemental chemical composition was evaluated by energy dispersive X-ray spectroscopy (EDS) coupled to the SEM system, allowing identification and distribution of the constituent elements of the analyzed materials.

Fourier transform infrared spectroscopy (FTIR) was employed to identify the functional groups present in the samples. The analyses were performed using a PerkinElmer Spectrum 65 FTIR spectrometer operating in the wavenumber range from 4000 to 600 cm^{-1} .

The optical properties of the composites were investigated by ultraviolet visible spectroscopy (UV-Vis). The analyses were conducted using a Kesvi UV Vis spectrophotometer, model K37, operating in the spectral range from 190 to 1100 nm .

Figure 1 presents a schematic diagram illustrating the complete preparation process of the photocatalyst, including graphene oxide (GO) synthesis, TiO_2 formation, and TiO_2 :GO composite production. The diagram was designed to provide a clear and reproducible overview of the experimental procedure. The schematic representation summarizes all critical synthesis parameters and processing steps, facilitating experimental reproducibility and providing a clear visualization of the methodology adopted in this study.

Using the absorbance curves and the linear fit obtained from reference standards, the methylene blue (MB) concentration in solution was quantitatively determined. This quantification enabled the evaluation of two key parameters for all reactors: degradation efficiency (DE) and degradation kinetics (k) [13,14]. Degradation efficiency (DE) quantifies the fraction of contaminant

removed from the solution during the degradation process, where higher DE values indicate a more effective process. Degradation efficiency was calculated according to Equation (1):

$$DE(\%) = \frac{C_0 - C_t}{C_0} \times 100 \quad (1)$$

Where C_0 represents the initial dye concentration in solution, expressed in mol L^{-1} or g L^{-1} , and C_t denotes the contaminant concentration at a given time t during the degradation process.

Degradation kinetics is also an important parameter for understanding how the contaminant degradation evolves. In this study, the degradation kinetics were described using a first-order kinetic model, expressed by Equation (2):

$$\ln\left(\frac{C_0}{C_t}\right) = kt \quad (2)$$

Where k is the apparent first-order rate constant, expressed in h^{-1} , and t is the irradiation or reaction time. The concentration of methylene blue was determined from absorbance values using a linear calibration curve obtained at 664 nm , according to the equation:

$$C = (1.4535 \pm 0.0210) \times 10^{-7} \text{ Abs} - (1.056 \pm 0.102) \times 10^{-6}$$

Where C is the concentration in mol L^{-1} . The calibration curve showed excellent linearity, with an adjusted coefficient of determination (Adj. R^2) of 0.9965 .

3. RESULT AND DISCUSSION

Figure 2 presents the X-ray diffraction patterns of the three analyzed samples: graphene oxide (GO), pure TiO_2 , and the composite containing 5 wt.% GO (TiO_2 :GOS), recorded in the 2θ range from 5° to 80° .

The diffraction pattern of exfoliated graphene oxide exhibits an intense and well-defined peak at 2θ approximately 10.8° , corresponding to an interplanar spacing of about 8.19 \AA , which is characteristic of the functionalized structure of GO [15]. This increase

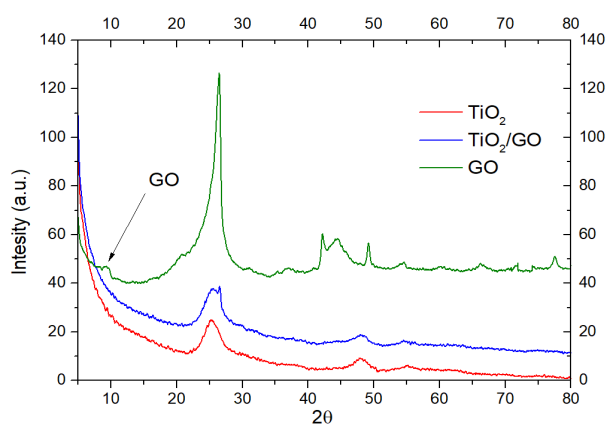


Figure 2. X ray diffraction patterns of graphene oxide (GO), pure TiO_2 , and the TiO_2 :GO5 composite, showing the characteristic GO peak and the predominance of the anatase phase in TiO_2 , as well as the preservation of the crystalline structure after graphene oxide incorporation.

in interlayer spacing is associated with the introduction of oxygen containing functional groups, such as hydroxyl, epoxy, and carboxyl groups, between the graphene layers, confirming the effective oxidation of the graphite precursor.

In addition, residual peaks are observed at approximately $2\theta = 26.4^\circ$, 42.3° , 44.4° , and 54.4° , indicating the presence of graphitic structures. The diffraction pattern of pure TiO_2 exhibits well-defined reflections at approximately $2\theta = 25.3^\circ$, 37.8° , 48.0° , 54.0° , and 62.7° , in agreement with the crystallographic standard JCPDS No. 01-071-1168, confirming the predominance of the anatase phase [16].

The identification of anatase is particularly relevant, as the photocatalytic performance of TiO_2 is strongly phase-dependent. Among its polymorphs, anatase is widely recognized as the most active phase for the degradation of organic pollutants due to its favorable band structure, reduced electron–hole recombination rate, and higher surface reactivity. Therefore, confirming its predominance allows a direct correlation between crystalline structure and the degradation efficiencies and kinetic constants obtained. Moreover, since the synthesis was conducted under relatively low-temperature conditions, the formation of anatase demonstrates that the adopted chemical route can produce the most photocatalytically active phase without requiring high thermal energy input. No reflections associated with rutile or brookite were detected, indicating the selectivity of the synthesis route toward anatase formation.

For the TiO_2 :GO5 nanocomposite, a diffraction profile similar to that of pure TiO_2 is observed, with preservation of the main anatase reflections, indicating that GO incorporation did not significantly alter the crystalline structure of the semiconductor [17]. An additional peak at approximately $2\theta = 26.4^\circ$ is detected and attributed to the graphitic structure of GO, confirming its presence in the composite. The absence of the characteristic GO peak at approximately $2\theta = 10.8^\circ$ suggests good dispersion of graphene oxide within the TiO_2 matrix, possibly due to interfacial interac-

tions between TiO_2 nanoparticles and GO sheets, which disrupt the typical lamellar organization of GO.

A slight reduction in peak intensity and subtle broadening of TiO_2 reflections are observed in the composite, which may indicate a decrease in apparent crystallinity associated with interfacial interactions between the phases, without compromising structural integrity. The absence of additional crystalline peaks suggests that GO is mainly present in an amorphous or highly dispersed state and does not interfere with the TiO_2 crystalline framework.

Based on these results, the successful exfoliation of graphene oxide and the efficient formation of anatase TiO_2 in both the pure and composite samples are confirmed, with no evidence of secondary phase formation. The incorporation of GO, evidenced by graphitic reflections, may contribute to improved electronic properties by facilitating charge separation, which can enhance photocatalytic performance in the degradation of organic pollutants for water and wastewater treatment applications [18].

Figure 3 presents scanning electron microscopy images of GO, pure TiO_2 , and the TiO_2 :GO5 composite, obtained at a magnification of 10,000 \times .

The micrograph in Figure 3a (GO) reveals thin, overlapping sheet-like structures with a lamellar and wrinkled morphology, which are characteristic of graphene oxide. This morphology indicates successful exfoliation, resulting in well-defined two-dimensional layers, as reported in the literature [19, 20]. According to Wu et al. (2022) [21], the high surface area-to-volume ratio of GO sheets favors interfacial interactions, making GO a suitable support material in composite systems. Review studies further emphasize that the combination of high surface area and abundant surface functional groups makes GO particularly attractive for structural composites and membrane-based applications [22, 23].

Figure 3b (pure TiO_2) shows micrometric agglomerates with average dimensions of approximately 6 μm . These agglomerates exhibit a predominantly rounded morphology and rough surface texture, indicating heterogeneous particle distribution. Smaller particles are observed within the agglomerates, which may correspond to anatase crystallites formed during synthesis. Hierarchical structures composed of nanometric anatase crystallites assembled into micrometric aggregates are often explored to combine high specific surface area with enhanced light scattering, benefiting photocatalytic and dye-sensitized solar cell applications [24].

Figure 3c (TiO_2 :GO5) evidences the coexistence of GO sheets and TiO_2 particles, confirming successful incorporation of the oxide into the carbonaceous matrix. Compared to pure TiO_2 , reduced agglomeration is observed, suggesting improved particle dispersion. This behavior may be attributed to interfacial interactions between TiO_2 nanoparticles and GO sheets, in which the two-dimensional structure of GO acts as a physical support that limits nanoparticle growth and aggregation [25].

Such improved dispersion is relevant for photocatalysis, as it increases interfacial contact between phases, enhances accessibility to active sites, and favors adsorption and surface reactions. According to Zhang et al. (2025) [26], intimate contact between TiO_2 and GO can broaden light absorption and improve pollutant adsorption capacity.

Figure 4 presents the energy-dispersive X-ray spectroscopy (EDS) spectra obtained for GO, pure TiO_2 , and the TiO_2 :GO5 composite during scanning electron microscopy analyses.

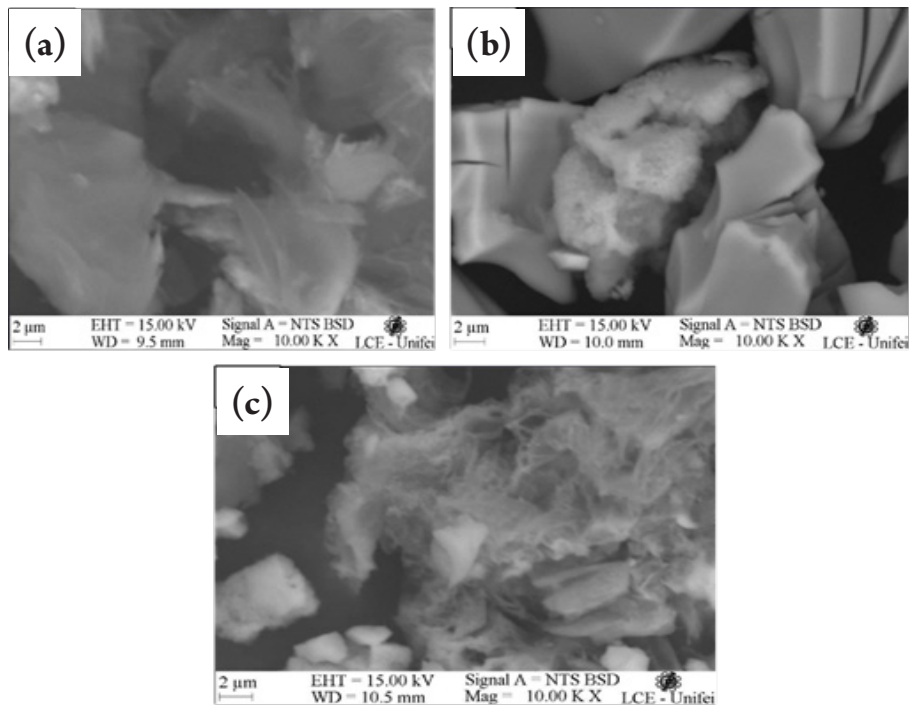


Figure 3. Scanning electron microscopy images of graphene oxide (GO) (a), pure titanium dioxide (TiO₂) (b), and the TiO₂:GO5 composite (c), recorded at a magnification of 10,000 times, highlighting morphological differences and the effect of graphene oxide incorporation on particle dispersion.

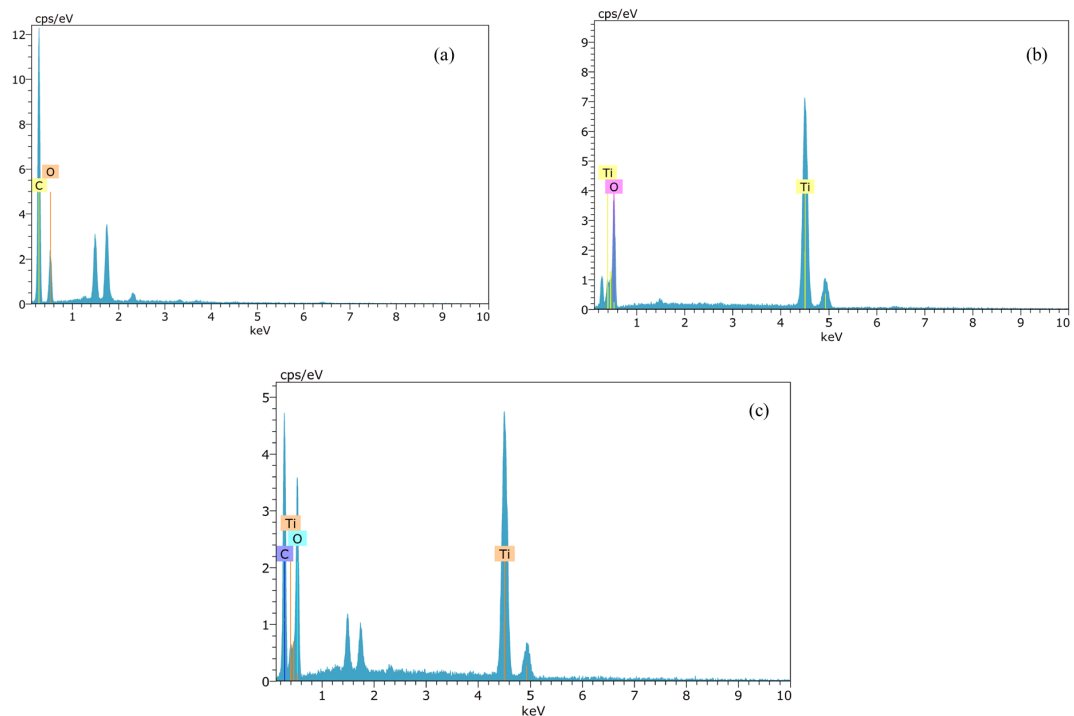


Figure 4. Energy dispersive X ray spectroscopy spectra of (a) graphene oxide (GO), (b) pure titanium dioxide (TiO₂), and the (c) TiO₂:GO5 composite, showing the elemental composition and confirming the successful incorporation of TiO₂ into the graphene oxide matrix.

The EDS spectrum of the GO sample (Figure 4) predominantly exhibits peaks associated with carbon (C) and oxygen (O), confirming the characteristic chemical composition of graphene oxide. Carbon is observed as the most intense peak, which is expected since GO retains the basal structure of graphene, composed mainly of carbon atoms, even after the oxidation process. The presence of oxygen, evidenced by a peak of lower intensity compared to carbon, is associated with the incorporation of oxygen containing functional groups, such as hydroxyl, epoxy, carbonyl, and carboxyl groups, on the surface and edges of the graphene sheets. These functional groups are responsible for the material functionalization and confer increased chemical reactivity and hydrophilicity to GO, favoring its interaction with inorganic phases, such as TiO_2 , in the formation of composite materials.

For the TiO_2 :GO5 composite, the EDS spectrum reveals the simultaneous presence of titanium (Ti), oxygen (O), and carbon (C), confirming the successful incorporation of titanium dioxide into the graphene oxide matrix. The detection of carbon together with the characteristic peaks of Ti and O provides clear evidence of composite formation, with no detectable introduction of foreign contaminants.

The relative intensity of the Ti peaks is lower than that observed for the pure TiO_2 sample, which can be attributed to the lower mass fraction of the metal oxide in the composite and to its dispersion over the GO sheets. The combined analysis of EDS and SEM results indicates that TiO_2 particles are well distributed on the GO surface, favoring efficient interfacial interactions between the phases. This interfacial interaction is particularly relevant for photocatalytic applications, as the presence of GO can act as an electron acceptor, reducing the recombination of photogenerated electron-hole pairs in TiO_2 . In addition, the absence of extraneous elements in the EDS spectra confirms that the functional performance of the composite is associated exclusively with the synergy between TiO_2 and GO.

For the pure TiO_2 sample, the EDS spectrum presents well-defined peaks corresponding to titanium (Ti) and oxygen (O), with no significant signals from impurities, indicating high purity of the synthesized material. The qualitative ratio between Ti and O peaks is consistent with the expected stoichiometry of titanium dioxide. The absence of residual elements further reinforces the efficiency of the synthesis route employed, in agreement with the X-ray diffraction results, which indicate the predominant formation of the anatase phase. Overall, the EDS results corroborate the structural and morphological analyses, confirming the purity of the samples, the effective formation of the TiO_2 :GO5 composite, and the chemical compatibility between the phases, which are fundamental aspects for the photocatalytic performance of the material.

Figure 5 presents the FTIR spectra of the TiO_2 and TiO_2 :GO materials, obtained to identify the functional groups present and to evaluate the chemical interactions established between graphene oxide (GO) and titanium dioxide.

The FTIR spectrum of TiO_2 shows a broad band in the region between 3200 and 3600 cm^{-1} , which is attributed to the stretching vibrations of hydroxyl groups ($^*\text{OH}$) adsorbed on the surface, as well as to the presence of physically adsorbed water molecules, reflecting the interaction of water with the material surface. Intense bands observed below 800 cm^{-1} correspond to the stretching vibrations of Ti-O-Ti bonds, which are characteristic of the TiO_2

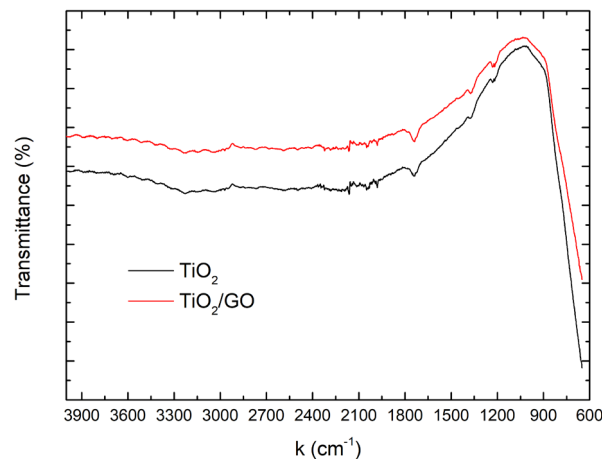


Figure 5. FTIR spectra of pure TiO_2 and the TiO_2 :GO composite, highlighting the characteristic vibrational bands and the effect of graphene oxide incorporation on surface functional groups and interfacial interactions.

crystalline network, particularly the anatase phase, widely recognized for its high photocatalytic activity. FTIR studies indicate that the density of surface hydroxyl groups can significantly modulate the photocatalytic properties of TiO_2 , since these groups act as active sites for adsorption and for the generation of hydroxyl radicals, which are essential for photocatalytic processes [27].

For the TiO_2 :GO material, in addition to the bands typical of TiO_2 , additional signals associated with the oxygen containing functional groups of GO are observed. Notably, a band around 3400 cm^{-1} is related to the stretching of hydroxyl groups, a band near 1720 cm^{-1} is attributed to the stretching of carbonyl groups ($\text{C}=\text{O}$) from carboxylic functionalities, and a band around 1620 cm^{-1} is associated with vibrations of the aromatic $\text{C}=\text{C}$ skeleton of GO and or with the bending deformation of adsorbed water molecules. Furthermore, bands in the range between 1050 and 1250 cm^{-1} can be related to C-O stretching vibrations from epoxy and alkoxy groups, confirming the presence of graphene oxide in the composite matrix [28].

Comparison between the spectra reveals shifts and intensity changes in some TiO_2 bands after GO incorporation, especially in the low-frequency region. These modifications indicate the occurrence of chemical and interfacial interactions between the oxygenated functional groups of GO and the TiO_2 surface. The presence of a band or shoulder in the region between approximately 800 and 1000 cm^{-1} in the TiO_2 :GO composite can be associated with the formation of Ti-O-C bonds, suggesting chemical anchoring of TiO_2 onto the GO sheets rather than a simple physical mixture [29].

These chemical interactions are particularly relevant for the photocatalytic activity of the TiO_2 :GO material, since the formation of Ti-O-C bonds and the strong interfacial interaction favor the transfer of photogenerated charges, reducing electron-hole recombination and consequently improving photocatalytic performance. In addition, the functional groups of GO contribute to an increase in surface area and enhance the adsorption of reactive species, further promoting photocatalytic efficiency [30, 31]

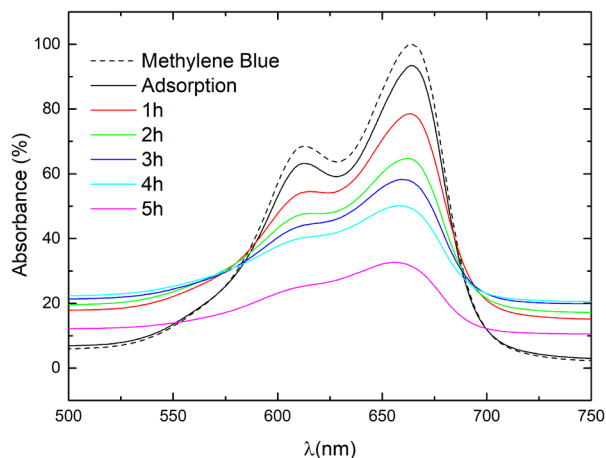


Figure 6. Absorbance spectra of the methylene blue (MB) solution at different irradiation times under UVC light in the presence of the TiO_2 :GO composite, showing the progressive decrease in absorbance associated with photocatalytic degradation.

The photocatalytic performance of the TiO_2 :GO composite and pure TiO_2 under UVC irradiation was evaluated through the degradation of methylene blue, as shown in Figures 5 and 6, respectively. A comparative analysis of these results provides important insights into the role of graphene oxide incorporation, particularly considering the relatively low calcination temperature employed during TiO_2 synthesis.

For the TiO_2 :GO composite, Figure 6 shows a pronounced and continuous decrease in the absorbance intensity of methylene blue in the spectral region between 660 nm and 665 nm as the irradiation time increases from 1 h to 5 h. An initial reduction in absorbance is observed even before irradiation, indicating significant adsorption of the dye on the composite surface.

This behavior is associated with the high specific surface area of graphene oxide and the abundance of oxygen containing functional groups, which promote strong interactions with the aromatic structure of methylene blue through electrostatic attraction and π - π interactions [18]. Upon UVC irradiation, the progressive decrease in absorbance confirms an efficient photocatalytic degradation process, with low residual absorbance after 5 h.

In contrast, Figure 7 shows the absorbance spectra obtained during methylene blue degradation in the presence of pure TiO_2 under identical irradiation conditions. Although a gradual decrease in absorbance at approximately 664 nm is observed with increasing irradiation time, the overall reduction is less pronounced when compared to the TiO_2 :GO composite. This behavior can be attributed to the lower crystallinity of the pure TiO_2 sample, which was calcined at relatively low temperature. Insufficient thermal treatment may lead to a higher density of structural defects and surface states, which act as recombination centers for photogenerated electron hole pairs, limiting the formation of reactive species such as hydroxyl radicals and superoxide anions [32]. The incorporation of graphene oxide mitigates these limitations by promoting efficient interfacial charge separation. Due to the intimate contact between TiO_2 particles and GO sheets, graphene oxide acts as an electron acceptor and transport pathway, reducing electron-hole

recombination and enhancing photocatalytic activity [33]. This synergistic effect allows high photocatalytic activity to be achieved without the need for high-temperature calcination, representing a significant advantage from energetic and economic perspectives.

In addition, the TiO_2 :GO composite exhibits enhanced adsorption of methylene blue before irradiation, increasing the local concentration of the pollutant near the photocatalytically active sites. This adsorption, combined with improved charge transfer dynamics, explains the superior degradation performance observed for the composite system [34]. The absence of significant shifts in the maximum absorbance peak for both systems suggests that the degradation process occurs predominantly through mineralization of the dye, rather than through reversible structural transformations.

The moderate increase in degradation rate suggests improved interfacial charge transfer promoted by GO incorporation. This finding highlights the potential of the TiO_2 :GO composite as a cost-effective and energy-efficient photocatalyst for wastewater treatment applications, where reducing synthesis temperature without compromising performance is a critical advantage. Figure 8 shows the degradation efficiency of methylene blue as a function of irradiation time for the TiO_2 and TiO_2 :GO systems, expressed by the dimensionless ratio C/C_0 , where C_0 is the initial dye concentration and C is the concentration at irradiation time t .

At the initial time (0 h), $C/C_0 = 1$ for both systems. After 1 h of irradiation, the values decrease to approximately 0.83 (TiO_2) and 0.82 (TiO_2 /GO), indicating that about 17–18% of the dye has already been degraded. At 2 h, the values reach approximately 0.68 (TiO_2) and 0.66 (TiO_2 /GO), showing continuous progress of the process. After 3 h, $C/C_0 \approx 0.60$ (TiO_2) and 0.58 (TiO_2 /GO) are observed, while at 4 h the values decrease to approximately 0.50 (TiO_2) and 0.49 (TiO_2 /GO). At the end of 5 h, the relative concentration reaches about 0.29 for TiO_2 and 0.28 for TiO_2 /GO. Both photocatalysts promote a progressive degradation of the dye over the irradiation period, as evidenced by the continuous decrease in

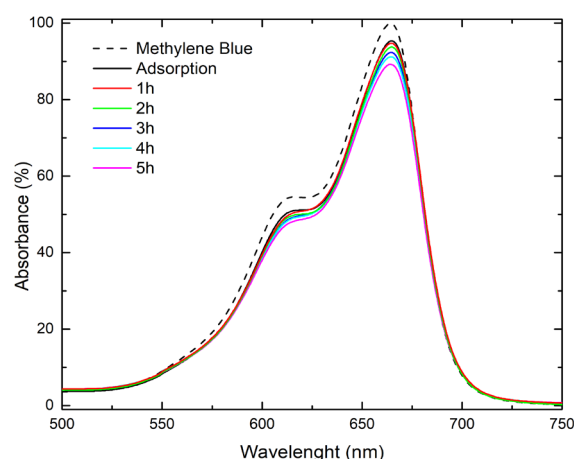


Figure 7. Absorbance spectra of the methylene blue (MB) solution recorded between 500 and 750 nm at different irradiation times under UVC light in the presence of pure TiO_2 , showing the progressive decrease in absorbance associated with photocatalytic degradation of the dye.

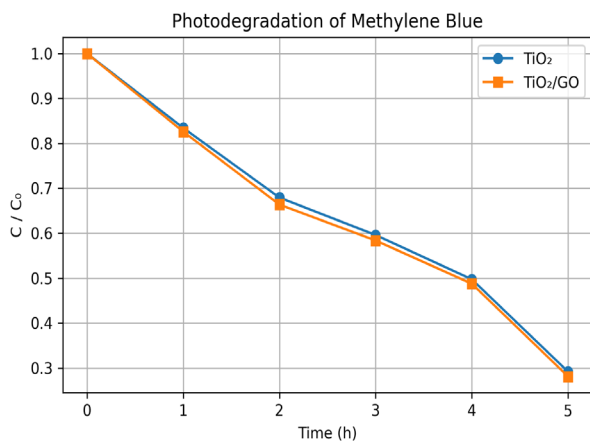


Figure 8. Photocatalytic degradation efficiency of methylene blue expressed as C/C_0 as a function of irradiation time for pure TiO_2 and the TiO_2 :GO composite under UVC irradiation.

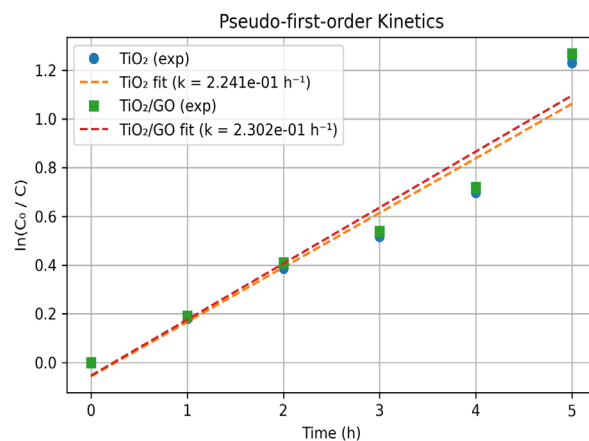


Figure 9. Pseudo-first-order kinetic plots for methylene blue degradation under UVC irradiation in the presence of pure TiO_2 and the TiO_2 :GO composite, used to determine the apparent rate constants k .

the C/C_0 ratio. After 5 h of irradiation, both systems reach high degradation levels, with final C/C_0 values close to 0.30, corresponding to removal efficiencies higher than 70 percent. These results confirm the effective photocatalytic activity of both materials under the applied experimental conditions.

These results confirm that both materials exhibit high photocatalytic activity. However, the composite shows slightly superior performance during the entire experiment, suggesting a synergistic effect between TiO_2 and GO. The improved performance can be attributed to enhanced electron transport and reduced recombination rates, leading to more efficient generation of reactive oxidative species responsible for dye degradation.

A comparative analysis reveals that the TiO_2 :GO composite exhibits slightly lower C/C_0 values than pure TiO_2 throughout most of the experimental time, particularly between 2 h and 4 h of irradiation, indicating a marginally superior photocatalytic performance. This enhancement can be attributed to the presence of graphene oxide, which acts as an electron acceptor and transport medium, reducing the recombination of photogenerated electron-hole pairs in TiO_2 and consequently favoring the formation of reactive species such as hydroxyl radicals and superoxide species, which are responsible for dye oxidation [33].

In addition to improved charge separation, graphene oxide contributes to increased surface area and enhanced adsorption of methylene blue on the photocatalyst surface, intensifying the interaction between the pollutant molecules and the active sites [35]. This combined effect of improved adsorption and more efficient charge transfer explains the higher degradation efficiency observed for the TiO_2 :GO composite, particularly at shorter irradiation times.

Although the difference between the two systems is less pronounced at the final irradiation time, the kinetic trend observed throughout the process clearly indicates that the TiO_2 :GO composite presents superior photocatalytic efficiency, especially during the initial stages of degradation. These results demonstrate that the incorporation of graphene oxide is an effective strategy to enhance the photocatalytic performance of TiO_2 , even under low temperature calcination conditions, reinforcing the potential of this composite

material for application in the photocatalytic treatment of aqueous effluents. Figure 9 presents the pseudo-first-order kinetic fitting for methylene blue degradation using the TiO_2 and TiO_2 :GO photocatalysts, obtained from the linear relationship between $\ln(C_0/C)$ and irradiation time.

The experimental data exhibited strong linear correlation for both systems, indicating that a pseudo-first-order kinetic model adequately describes the degradation process. From the linear fitting, the apparent rate constants were determined, yielding $k = 2.241 \times 10^{-1} \text{ h}^{-1}$ for pure TiO_2 and $k = 2.302 \times 10^{-1} \text{ h}^{-1}$ for the TiO_2 :GO composite. The TiO_2 :GO system therefore exhibits a slightly higher kinetic constant than pure TiO_2 , indicating a higher degradation rate of methylene blue over time.

The increase in the k value for the TiO_2 :GO composite can be attributed to the synergistic interaction between TiO_2 and graphene oxide, which promotes more efficient separation and transport of photogenerated charges, reducing electron hole recombination [36]. As a consequence, a higher availability of reactive oxidizing species, such as hydroxyl radicals and superoxide species, is achieved, enhancing the degradation of methylene blue. In addition, the higher surface area and adsorption capacity provided by graphene oxide intensify the interaction between the pollutant molecules and the active sites of the photocatalyst, further contributing to the improved kinetic performance.

Although the difference between the k values is not large, the kinetic behavior clearly confirms the enhancement of photocatalytic performance promoted by graphene oxide incorporation into TiO_2 . These results are consistent with the degradation efficiency trends observed in Figures 5 to 7 and reinforce the potential of the TiO_2 :GO composite for application in photocatalytic treatment of aqueous effluents, particularly under low temperature synthesis and calcination conditions.

Overall, the combined results obtained from structural, morphological, chemical, optical, and photocatalytic analyses provide consistent evidence of the successful synthesis and enhanced performance of the TiO_2 :GO composite. X-ray diffraction confirmed the effective formation of the anatase phase in both pure TiO_2 and

the composite, while the absence of additional crystalline phases indicated good structural compatibility between TiO₂ and graphene oxide. Scanning electron microscopy and energy dispersive X-ray spectroscopy revealed improved dispersion of TiO₂ particles on the graphene oxide sheets, with homogeneous elemental distribution and no detectable contaminants. FTIR analysis demonstrated the presence of oxygen containing functional groups from graphene oxide and suggested the formation of interfacial Ti O C bonds, indicating strong chemical interaction between the phases.

The optical and photocatalytic evaluations further corroborated the advantages of graphene oxide incorporation. UV Vis absorbance measurements showed efficient degradation of methylene blue under UVC irradiation, with the TiO₂:GO composite exhibiting higher adsorption capacity and faster absorbance decay compared to pure TiO₂. Degradation efficiency and kinetic analyses confirmed that both systems were active photocatalysts, although the composite consistently presented superior performance, particularly at shorter irradiation times and in terms of apparent rate constant. Importantly, this enhanced activity was achieved despite the relatively low calcination temperature employed during TiO₂ synthesis, suggesting that graphene oxide effectively compensates for limitations associated with reduced crystallinity by promoting charge separation and suppressing electron-hole recombination.

Taken together, these results demonstrate that the TiO₂:GO composite enables efficient photocatalytic degradation of organic pollutants under mild synthesis conditions, highlighting its potential as a cost-effective and energy-efficient material for advanced water and wastewater treatment applications.

4. CONCLUSION

This work aimed to develop and evaluate photocatalytic materials based on titanium dioxide (TiO₂) and graphene oxide (GO) for application in the degradation of organic pollutants in water and wastewater treatment systems. The results demonstrated that the synthesis route employed was effective for obtaining exfoliated graphene oxide, TiO₂ predominantly in the anatase phase, and TiO₂:GO composites with adequate integration between the phases. The proposed synthesis route proved to be effective, as demonstrated by the photocatalytic performance results. The TiO₂:GO composite achieved methylene blue removal efficiencies higher than 70% after 5 h of UVC irradiation, reaching a final C/C₀ value close to 0.30. In addition, the degradation process followed pseudo-first-order kinetics with an apparent rate constant of $2.302 \times 10^{-1} \text{ h}^{-1}$, slightly superior to that of pure TiO₂ ($2.241 \times 10^{-1} \text{ h}^{-1}$). These quantitative results confirm that the adopted chemical synthesis method successfully produced a structurally integrated composite with enhanced photocatalytic activity, validating its effectiveness for advanced water treatment applications.

X ray diffraction analyses confirmed the formation of anatase TiO₂ and the successful incorporation of graphene oxide into the composite, with no evidence of secondary crystalline phase formation.

Scanning electron microscopy images showed that the presence of graphene oxide promoted a more homogeneous dispersion of TiO₂ particles, with a significant reduction in agglomeration compared to the pure TiO₂ material. The expected chemical composition of the samples was confirmed by energy dispersive X ray spec-

troscopy, with no detection of relevant impurities, indicating the efficiency and reliability of the synthesis process.

FTIR spectra revealed the presence of characteristic functional groups of graphene oxide and indicated chemical interactions between TiO₂ and graphene oxide, possibly associated with the formation of Ti O C bonds. These interfacial interactions play an important role in enhancing charge transfer processes, reducing the recombination of photogenerated electron hole pairs and contributing to improved photocatalytic performance.

Photodegradation experiments using methylene blue as a model pollutant demonstrated that both pure TiO₂ and TiO₂:GO composites are photocatalytically active under UVC irradiation. However, the composite containing 5 percent by mass of graphene oxide, TiO₂:GOS, exhibited superior performance, with higher dye removal efficiency over time. This enhancement is attributed to the increased initial adsorption capacity provided by graphene oxide and to the more effective utilization of photogenerated charge carriers.

Overall, the results indicate that modification of TiO₂ with graphene oxide is an effective strategy to enhance its photocatalytic properties. The TiO₂:GOS composite presented the best balance between structural characteristics, interfacial interactions, and photocatalytic performance, identifying it as the most promising material for application in advanced water and wastewater treatment processes, particularly under low temperature synthesis and calcination conditions.

ACKNOWLEDGEMENTS

The authors would like to express their gratitude for the financial support from the Minas Gerais Research Foundation (FAPEMIG – Grant APQ-03495).

CREDIT AUTHOR STATEMENT

Caroliny Fernandes de Carvalho: Writing – original draft, Data curation, Methodology. **Adhimar Flávio Oliveira:** Supervision, Writing – original draft, Methodology. **Maria Elena Leyva Gonzalez:** Resources, Data curation. **Vander Alkmin dos Santos Ribeiro:** Writing – review and editing, Investigation. **Celso Henrique Correa Carvalho:** Data curation, Methodology.

DECLARATIONS

Conflict of interest The authors declare that they have no known competing financial interests or personal relationships that could have appeared to influence the work reported in this paper.

AVAILABILITY OF DATA

The All data supporting the findings of this study are included within the manuscript. Any additional data related to this work is available from the corresponding author upon reasonable request.

REFERENCES

- [1] Morin, N., Eric, C., Marc, L., Ana, F., & Lado, R. (2021). Removal of emerging contaminants from wastewater using advanced treatments: A review. *Environmental Chemistry Letters*, 20, 1333–1375. <https://doi.org/10.1007/s10311-021-01379-5>.
- [2] Pratap, B., Kumar, S., Nand, S., Azad, I., Bharagava, R. N., Romanholo Ferreira, L. F., & Dutta, V. (2023). Wastewater generation and treatment by various eco-friendly technologies: Possible health hazards and further reuse for environmental safety. *Chemosphere*, 313, 137547. <https://doi.org/10.1016/j.chemosphere.2022.137547>.
- [3] Saravanan, A., Senthil Kumar, P., Jeevanantham, S., Karishma, S., Tajsabreen, B., Yaashikaa, P. R., & Reshma, B. (2021). Effective water/wastewater treatment methodologies for toxic pollutants removal: Processes and applications towards sustainable development. *Chemosphere*, 280, 130595. <https://doi.org/10.1016/j.chemosphere.2021.130595>.
- [4] Zhu, Q., Li, X., & Song, F. (2025). Emerging contaminants in natural and engineered water environments: Environmental behavior, ecological effects and control strategies. *Water*, 17(9), 1329. <https://doi.org/10.3390/w17091329>.
- [5] Paiu, M., Lutic, D., Favier, L., & Gavrilescu, M. (2025). Heterogeneous photocatalysis for advanced water treatment: Materials, mechanisms, reactor configurations, and emerging applications. *Applied Sciences*, 15(10), 5681. <https://doi.org/10.3390/app15105681>.
- [6] Friedmann, D. (2022). A general overview of heterogeneous photocatalysis as a remediation technology for wastewaters containing pharmaceutical compounds. *Water*, 14(21), 3588. <https://doi.org/10.3390/w14213588>.
- [7] Chauke, N. M., Ngqalakwezi, A., & Raphulu, M. (2025). Transformative advancements in visible-light-activated titanium dioxide for industrial wastewater remediation. *International Journal of Environmental Science and Technology*, 22, 8521–8552. <https://doi.org/10.1007/s13762-025-06397-2>.
- [8] Pelosato, R., Bolognino, I., Fontana, F., & Sora, I. N. (2022). Applications of heterogeneous photocatalysis to the degradation of oxytetracycline in water: A review. *Molecules*, 27(9), 2743. <https://doi.org/10.3390/molecules27092743>.
- [9] Ortelli, S., Faccani, L., Ercolani, E., Zanoni, I., Artusi, C., Blosi, M., Albonetti, S., & Costa, A. L. (2025). Design and properties of titanium dioxide/graphene oxide composites exploitable in wastewater treatments. *Water*, 17(12), 1809. <https://doi.org/10.3390/w17121809>.
- [10] Costa, M. C. F., Marangoni, V. S., Ng, P. R., Nguyen, H. T. L., Carvalho, A., & Castro Neto, A. H. (2021). Accelerated synthesis of graphene oxide from graphene. *Nanomaterials*, 11(2), 551. <https://doi.org/10.3390/nano11020551>.
- [11] Purabgola, A., Mayilswamy, N., & Kandasubramanian, B. (2022). Graphene-based TiO₂ composites for photocatalysis and environmental remediation: Synthesis and progress. *Environmental Science and Pollution Research*, 29, 32305–32325. <https://doi.org/10.1007/s11356-022-18983-9>.
- [12] Pereira, E. L., Gama, A., González, M. E. L., & Oliveira, A. F. (2023). Synergistic electrochemical method to prepare graphene oxide/polyaniline nanocomposite. *Polímeros*, 33, e20220102. <https://doi.org/10.1590/0104-1428.20220102>.
- [13] Pinton, J. H. B., Oliveira, A. F., Huanca, D. R., & Mohallem, N. D. S. (2024). Development of an automated and cost-effective apparatus for sol–gel solution deposition using spray coating technique and its application for TiO₂-based photocatalytic films. *Materials Chemistry and Physics*, 318, 129213. <https://doi.org/10.1016/j.matchemphys.2024.129213>.
- [14] Pinton, J. H. B., Carvalho, C. H. C., Huanca, D. R., Gomes, A. M. C., Mohallem, N. D. S., & Oliveira, A. F. (2025). Optimization and stability of spray-coated titanium dioxide thin films: Influence of calcination on photocatalytic properties for pollutant treatment. *Journal of Electronic Materials*, 54, 7914–7926. <https://doi.org/10.1007/s11664-025-12108-x>.
- [15] Aliyev, E., Filiz, V., Khan, M. M., Lee, Y. J., Abetz, C., & Abetz, V. (2019). Structural characterization of graphene oxide: Surface functional groups and fractionated oxidative debris. *Nanomaterials*, 9(8), 1180. <https://doi.org/10.3390/nano9081180>.
- [16] Kobir, M. M., Tabassum, S., Ahmed, S., Sadia, S. I., & Alam, M. A. (2024). Crystallographic benchmarking on diffraction pattern profiling of polymorphs TiO₂ by WPPF for pigment and acrylic paint. *Archive of Current Research International*, 24, 62–70. <https://doi.org/10.9734/acri/2024/v24i1623>.
- [17] Alsultani, M. J., & Alias, M. F. A. (2025). Impact of graphene oxide concentration and anthocyanin dye on the structural, morphological and optical properties of GO:TiO₂ thin films. *Iraqi Journal of Science*, 66, 2336–2349. <https://doi.org/10.24996/ij.s.2025.66.6.12>.
- [18] Kong, E. D. H., Chau, J. H. F., Lai, C. W., Khe, C. S., Sharma, G., Kumar, A., Siengchin, S., & Sanjay, M. R. (2022). GO/TiO₂-related nanocomposites as photocatalysts for pollutant removal in wastewater treatment. *Nanomaterials*, 12(19), 3536. <https://doi.org/10.3390/nano12193536>.
- [19] Liu, Z., Fan, J., Xue, J., & Guo, F. (2025). Drying and film formation processes of graphene oxide suspension on nonwoven fibrous membranes with varying wettability. *Surfaces*, 8(2), 39. <https://doi.org/10.3390/surfaces8020039>.
- [20] Park, J., Rahman, M. M., Ahn, S. J., & Lee, J. J. (2025). Phase transitions and morphology control of Langmuir–Blodgett films of graphene oxide. *Journal of Colloid and Interface Science*, 684, 215–224. <https://doi.org/10.1016/j.jcis.2025.01.044>.
- [21] Wu, Q., Yang, X., He, J., Ye, Z., Liu, Q., Bai, H., & Zhu, J. (2022). Improved interfacial adhesion of epoxy composites by grafting porous graphene oxide on carbon fiber. *Applied Surface Science*, 573, 151605. <https://doi.org/10.1016/j.apsusc.2021.151605>.
- [22] Sharma, H., Kumar, A., Rana, S., & Guadagno, L. (2022). An overview on carbon fiber-reinforced epoxy composites: Effect of graphene oxide incorporation on composites performance. *Polymers*, 14(8), 1548. <https://doi.org/10.3390/polym14081548>.
- [23] Wang, F., Qiao, W., Guo, W., Li, Z., & Cai, X. (2022). Fabrication and functionalization of biocompatible carboxymethyl chitosan/gelatin membranes via anodic electrophoretic deposition. *RSC Advances*, 12, 5677–5685. <https://doi.org/10.1039/D1RA09231F>.

- [24] Alduraibi, M., Hezam, M., Al-Ruhaimi, B., El-Toni, A. M., Algarni, A., Abdel-Rahman, M., Qing, W., & Aldwayyan, A. (2020). Rapid room-temperature synthesis of mesoporous TiO₂ sub-microspheres and their enhanced light harvesting in dye-sensitized solar cells. *Nanomaterials*, 10(3), 413. <https://doi.org/10.3390/nano10030413>.
- [25] Tao, S., & Xiaojuan, J. (2021). Simple fabrication of RGO/TiO₂ nanocomposite with homogeneous dispersion. *Journal of Physics: Conference Series*, 1750, 012056. <https://doi.org/10.1088/1742-6596/1750/1/012056>.
- [26] Zhang, X., Zhang, S., Mao, X., Liu, Y., Li, Y., Meng, W., Zhu, L., & Zhu, M. (2025). Composite aerogel membranes with well-dispersed nano M-TiO₂@GO for efficient photocatalysis. *Nanoscale Advances*, 7, 3889–3902. <https://doi.org/10.1039/D5NA00238A>.
- [27] Xiao, S. T., Wu, S. M., Dong, Y., Liu, J. W., Wang, L. Y., Wu, L., Zhang, Y. X., Tian, G., Janiak, C., Shalom, M., Wang, Y. T., Li, Y. Z., Jia, R. K., Bahnemann, D. W., & Yang, X. Y. (2020). Rich surface hydroxyl design for nanostructured TiO₂ and its hole-trapping effect. *Chemical Engineering Journal*, 400, 125909. <https://doi.org/10.1016/j.cej.2020.125909>.
- [28] Mathioudakis, G. N., Visvini, G. A., Sygellou, L., Soto Beobide, A., & Voyiatzis, G. A. (2025). Comparative in-depth investigation of benchmark graphene oxides in the perspective of their integration into industrial production processes. *Nanomaterials*, 15(13), 980. <https://doi.org/10.3390/nano15130980>.
- [29] Xiong, N., Guo, Y., Nie, Y., Yao, Y., Ying, Z., Zhang, W., Liu, R., Wu, X., Zhou, H., Zhou, L., Wang, Y., He, J., & Yan, L. (2025). An efficient photocatalytic material, rGO–TiO₂, that can be industrially produced: Fabrication and structural characterization. *Water*, 17(2), 161. <https://doi.org/10.3390/w17020161>.
- [30] Yadav, A., Yadav, M., Gupta, S., Popat, Y., Gangan, A., Chakraborty, B., Ramaniah, L. M., Fernandes, R., Miotello, A., Press, M. R., & Patel, N. (2019). Effect of graphene oxide loading on TiO₂: Morphological, optical, interfacial charge dynamics. *Carbon*, 143, 51–62. <https://doi.org/10.1016/j.carbon.2018.10.090>.
- [31] Prabhakarao, N., Rao, T. S., Lakshmi, K. V. D., Divya, G., Jaishree, G., Raju, I. M., & Alim, S. A. (2021). Enhanced photocatalytic performance of Nb-doped TiO₂/reduced graphene oxide nanocomposites over rhodamine B dye under visible light illumination. *Sustainable Environment Research*, 31, 10. <https://doi.org/10.1186/s42834-021-00110-x>.
- [32] Nasr, M., Eid, C., Habchi, R., Miele, P., & Bechelany, M. (2018). Recent progress on titanium dioxide nanomaterials for photocatalytic applications. *ChemSusChem*, 11, 3023–3047. <https://doi.org/10.1002/cssc.201800874>.
- [33] Sewela, T., Ocaya, R. O., & Malevu, T. D. (2025). Recent insights into the transformative role of graphene-based/TiO₂ electron transport layers for perovskite solar cells. *Energy Science & Engineering*, 13, 4–26. <https://doi.org/10.1002/ese3.1878>.
- [34] Van Bao, H., Dat, N. M., Giang, N. T. H., Thinh, D. B., Tai, L. T., Trinh, D. N., Hai, N. D., Khoa, N. A. D., Huong, L. M., Nam, H. M., Phong, M. T., & Hieu, N. H. (2021). Behavior of ZnO-doped TiO₂/rGO nanocomposite for water treatment enhancement. *Surfaces and Interfaces*, 23, 100950. <https://doi.org/10.1016/j.surfin.2021.100950>.
- [35] Farghaly, A., Maher, E., Gad, A., & El-Bery, H. (2024). Synergistic photocatalytic degradation of methylene blue using TiO₂ composites with activated carbon and reduced graphene oxide: A kinetic and mechanistic study. *Applied Water Science*, 14, 286. <https://doi.org/10.1007/s13201-024-02286-0>.
- [36] Gillespie, P. N. O., & Martsinovich, N. (2019). Origin of charge trapping in TiO₂/reduced graphene oxide photocatalytic composites: Insights from theory. *ACS Applied Materials & Interfaces*, 11, 31909–31922. <https://doi.org/10.1021/acsami.9b09235>.